COMPDYN 2015
5th ECCOMAS Thematic Conference on
Computational Methods in Structural Dynamics and Earthquake Engineering
M. Papadrakakis, V. Papadopoulos, V. Plevris (eds.)
Crete Island, Greece, 25–27 May 2015

PROBABILISTIC FATIGUE ANALYSIS OF OFFSHORE WIND TURBINES

Dimitrios V. Bilionis[1], **Dimitrios Vamvatsikos**[2]

[1] PhD Candidate
Institute of Steel Structures, School of Civil Engineering, National Technical University of Athens
Zografou Campus, Iroon Polytechneiou 9, 15780 Zografou, Athens, Greece
e-mail: dimbilionis@gmail.com

[2]Lecturer
Institute of Steel Structures, School of Civil Engineering, National Technical University of Athens
Zografou Campus, Iroon Polytechneiou 9, 15780 Zografou, Athens, Greece
e-mail: divamva@mail.ntua.gr

Keywords: Offshore Wind Turbine, Monopile Design, Fatigue, Aegean Sea

Abstract. *Wind Turbines constitute a sustainable and effective solution for the production of energy using wind power. Offshore wind turbines especially are becoming of special interest. However, their design poses great challenges, since an offshore structure is subject to combined wind and wave dynamic loading that is characteristic of the site of installation. The purpose of this paper is to provide a case study of fatigue life assessment for the cross-section at mudline (foundation) of a standard offshore wind turbine with a monopile design, under a probabilistic framework and assuming the thickness of the examined cross-section as the design variable. Two potential sites of construction in the Aegean Sea of Greece were examined. A probabilistic approach was employed in order to determine the fatigue life based on anemological data at each of the two sites of interest. At its basis is an extensive Monte Carlo simulation of wind (velocity) and wave (height, period) characteristics. The results show the dependence of fatigue life on the local wind and wave conditions, the cross-section geometry (i.e. the thickness of the foundation's pile) and the welded connection detail. All in all, the more benign conditions in the Aegean allow simpler connection details and smaller thickness of foundation pile's cross-section to still have acceptable performance.*

1 INTRODUCTION

Wind turbines constitute a sustainable and effective solution for the production of energy using wind power. Wind turbines may be constructed either in land areas (onshore) or in sea areas (offshore). Offshore wind turbines are becoming of special interest in recent years. Although an offshore wind turbine usually starts with a higher initial cost, it can outweigh a similar onshore one during its service life in a number of aspects such as: higher productivity due to stronger winds over sea areas, larger available installation areas and lower (or even non-existent) public nuisance. The latter is especially important in countries such as Greece where protracted court battles have hindered most onshore wind farms, inflicting substantial cost and crippling delays.

A wind turbine could be considered as a structure that lies between a civil engineering structure and a machine [1]. In specific, a wind turbine consists of structural elements (tower, substructure etc.) and a number of electrical and machine components with a control system (gear box, drivetrain etc.). Under a civil engineering perspective, the main components of a wind turbine could be considered the tower and the substructure system. The tower is the element on the top of which the mechanical parts of the wind turbine, such as the nacelle and the blades, are installed. The tower is made of steel and has a circular cross-section. It is usually tapered i.e. the cross-section size (e.g. diameter, thickness etc.) decreases with height, typically in a linear fashion. The tower is connected to the substructure, i.e., the part of the wind turbine that is submerged in the water. The substructure may be founded directly in the seabed or based on a floating platform. This type of the substructure's foundation usually distinguishes an offshore wind turbine into two categories, namely fixed and floating. Fixed wind turbines are used especially in sites of low or medium depths, while the construction of a floating wind turbine is cost-effective in the case of deep waters. The most common type of design for fixed wind turbines, which is used for depths up to 30 meters, is the monopile. This is probably the simplest structural concept, where the tower is connected (directly or via a transition piece) to a pile that has been founded at the seabed.

Regardless of the type of an offshore wind turbine, both structure and substructure are subject to dynamic combinations of wind and wave loads with a wide range of frequencies. This fact may raise critical issues during the turbine's service life in terms of fatigue and power efficiency [2]. For this reason, special focus should be devoted on the appropriate analysis and assessment of the dynamic combination of loads during the design phase. Furthermore, since wind turbines are complicated structures including a number of different components, reliability analysis considering consistent reliability levels and taking into account the dynamic nature of loads has received considerable attention by researchers [1, 3]. However, a great challenge in the above analysis is posed by the stochastic nature of the main loading mechanisms, namely wind and wave, as their characteristics tend to vary rapidly. Their stochasticity mainly depends on the climate at the area of construction. Thus, one could say that the design of an offshore wind turbine is a highly site-specific process. For this reason, the use of accurate site anemological and wave data is essential.

As far as the loads are concerned, the aforementioned stochasticity affects their magnitude and also subjects the structure to cyclic stresses making its components vulnerable to fatigue damage. Furthermore, they affect the overall performance and energy output. Research efforts are currently under way to incorporate climate information and relate it directly to the calculation of fatigue damage [4] or the assessment of performance [5]. However the stochastic nature of the wind and waves, as physical phenomena, makes such an analysis very complicated and advanced methods from statistics and probability theory need to be incorporated.

The purpose of this paper is to provide a case study of a probabilistic fatigue life assessment for a standard offshore wind turbine located in the Aegean Sea of Greece. In specific, a fixed offshore wind turbine with a monopile foundation is studied. Two potential sites of construction, one in the north part and another in the south part of Aegean, with different wind and wave characteristics, are considered. For both sites dynamic loading analysis is performed and the corresponding fatigue damage of the pile's cross-section at the mudline of the structure is calculated for different wind-wave states. The estimation of the expected fatigue life is made by incorporating Monte Carlo simulation. Furthermore, the thickness of the cross-section is examined as the design variable. Thus, estimations of the expected fatigue annual damage and corresponding life are made for a range of values of thickness and inferences about the influence of this parameter to fatigue life are made for both sites.

2 THE WIND TURBINE MODEL

The National Renewable Energy Laboratory (NREL) 5MW Baseline Wind Turbine was selected as a standard offshore wind turbine for this study. The rated power is 5 MW. The tower of the turbine is tapered and of steel circular hollow cross-section. The base diameter is 6.00 m and the thickness 27 mm, while the top diameter is 3.87 m with a thickness of 19mm. The height of the tower at its top point (where the nacelle is based) is at 87.60 m from the Mean Sea Level (MSL). The rotor has three blades. The rotor disk has a diameter of 126.00 m and its center (hub height) is located at 90.00 m from the MSL. The cut-in and cut-out wind speeds are 3 m/s and 25 m/s respectively. For additional details regarding the characteristics of the standard turbine the reader may refer to [6].The tower is connected to a monopile foundation via a transition piece (TP). The monopile is considered to be founded at a depth of 28 m. It has a steel circular hollow cross-section, 6.00 m in diameter. The thickness of the pile's cross-section in the standard model is 60 mm. The connection of the base of the tower to the transition piece is considered to be at 10.00 m of the MSL (Figure 1). Finally, a rigid type of foundation is assumed.

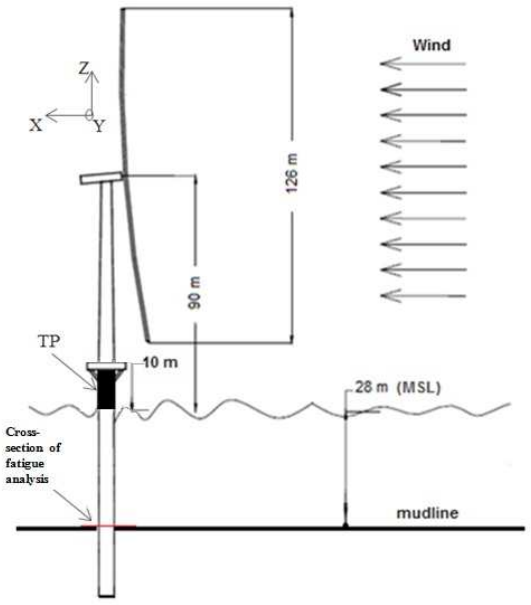

Figure 1: Wind turbine model (adapted from [7]).

3 THEORITICAL BACKGROUND

Design criteria and analysis guidance are provided by published standards. The analysis of offshore wind turbines is mainly based on the IEC 61400-3 standard [8]. It specifies the context for the assessment of external conditions and the design requirements to ensure the engineering integrity of the structure. The IEC standard also provides an appropriate level of protection from all hazards during the planned lifetime of an offshore wind turbine. In addition, the DNV standards [9] can also be used for the assessment of loads on marine structures subjected to wind, wave and current loading.

3.1 Loads

The assessment of wind loads is critical for the analysis of an offshore wind turbine. Although wind is essential for the operation and efficiency of a wind turbine, it is also the environmental factor with the greatest contribution to the loading of the structure. For the assessment of wind loads, time-series of wind speed at the hub height of the wind turbine are used. The time-series may have been developed according to specific spectrums (such as Kaimal or von Karman), based on the characteristic (average) value of a 10-minute wind speed. For this process appropriate software can be used, such as the TurbSim software developed by NREL [10] and adopted in this study. The wind time-series are then used as the input to calculate the values of reactions and deflections at the structure due to the wind. In this study, the authors used the FAST software [11].

Offshore wind turbines are also subject to wave loads which in some cases (e.g. in North Seas) may be very significant. Wave characteristics, such as the significant wave height (H_s) and peak spectral period (T_p), depend on the wind speed and the available sea length, or fetch, over which the wind transfers energy to the sea. Several methodologies and associated wave spectra are available for the calculation of the dynamic wave characteristics. A very widely used spectrum is JONSWAP [8, 9] that will also be our choice. A simplified method to transform wave characteristics into forces on a structure is the Morison equation [12]. This is a semi-empirical method for calculating the acting force on a body (e.g. a pile) that is submerged into moving water. The general form of the equation is as follows:

$$F = C_M \rho A \frac{du}{dt} + C_D \frac{1}{2} \rho D |u| u \tag{1}$$

where: D is the diameter of the member (pile), C_D and C_M are the drag and inertial coefficients respectively, ρ is the water density, A is the cross-sectional area and u is the water velocity relative to the body. The forces and the moments acting on the structure are then calculated by integrating the height-wise contributions of Eq. 1. For more details about the application of the Morison equation, the reader may refer to [9].

3.2 Fatigue

According to Eurocode 3 (EC3) [13], fatigue is considered as the damage in a member of a structure through crack initiation and/or crack propagation due to repeated stress fluctuations. Various standards have been published for the design of steel structures against fatigue. In the Eurocode series, part 1.9 of EC3 [13] provides the analysis context for fatigue design of steel structures. For the estimation of fatigue damage, time-series of stress history associated with the structural member of interest are needed. After those time-series are obtained, the stresses of various magnitudes should be grouped into groups of specific stress magnitude. Then, the

number of cycles (i.e. the frequency) of each group is counted. A very widely used approach for counting the number of cycles is the rainflow counting algorithm [14, 15].

By incorporating rainflow counting, the number of cycles of stress is calculated for each of the different stress amplitudes (or groups). Once the number of cycles for each group is specified, the corresponding fatigue damage can be estimated. In specific, if n_i is the number of cycles observed for stress group i, and N_{fi} is the number of cycles to failure for stress group i, the corresponding damage d_i is:

$$d_i = \frac{n_i}{N_{fi}} \tag{2}$$

The total damage D in a stress history of a specific length is then calculated by the following formula (Palmgren-Miner rule):

$$D = \sum_{i=1}^{k} d_i = \sum_{i=1}^{k} \frac{n_i}{N_{fi}} \tag{3}$$

The fatigue life of a structural member is the time until D reaches the maximum allowable value of 1. Assuming that D has been estimated for a representative enough interval of duration T_D over which its accumulation may be assumed to be stationary, a good estimate (assuming deterministic capacity) of the corresponding fatigue life is equal to T_D/D. For instance, if D is the mean annual fatigue damage of a member, the estimated fatigue life in years is equal to $1/D$ (in this case $T_D=1$).

4 CASE STUDIES FOR GREECE

4.1 Examined Sites

Offshore wind farms have been constructed and are in operation in the northern seas of Europe. On the other hand, none have been installed in the Mediterranean Sea. However, a number of projects are ongoing for examining the potential of design and installation of offshore wind farms by several Mediterranean countries [16]. In this paper, two case studies will be presented for the preliminary assessment of fatigue life for the cross-section at mudline of a standard offshore wind turbine with a monopile foundation for a range of thickness values of the cross-section. In specific, two different sites in the Aegean Sea of Greece were selected, shown in the map of Figure 2.

The first site is located on the North part of the Aegean, while the second site on the South part. Each has its own wind and wave characteristics, in large part due to the difference in the surrounding geography. For the case of the North site, due to the proximity of the mainland, significant difference in fetch (i.e. the uninterrupted length of water over which waves can develop) exists for the various wind directions, with the maximum appearing for a southern wind. In the case of the South site though, no much difference could be assumed between the different directions and a practically uniform fetch could be used for the analysis.

4.2 Analysis Process

For both sites of the study a similar process was followed for the estimation of the fatigue life. First, anemological data was obtained from the National Weather Service of Greece. A statistical analysis for specifying the major trends and the distribution of that data was performed. Given the relatively small fetch distances in the Aegean, the wind speed is reasonably

assumed to fully determine the wave state as well, something that would not be true, for example, in an ocean environment. Thus, the wave characteristics (significant wave height and peak period) were calculated based on the JONSWAP spectrum for each possible value of *local* wind speed. Finally, the joint probability density function (joint PDF) of wind speed *(U)* and significant wave height (H_s) were estimated, a process that will be discussed in more detail in the next section.

Figure 2: Map of Aegean Sea with the examined installation sites.

For the analysis of loads, time-series of wind speed at the hub height were simulated using the TurbSim software. In specific, time-series of 10-minute length, for a number of wind speed values, namely 3 m/s (cut-in), 5 m/s, 10 m/s, 15 m/s, 20 m/s, 25 m/s (cut-out) and 30 m/s (parked turbine) were developed. The aforementioned time-series along with the corresponding wave characteristics constituted the input for the FAST software, where a coupled (i.e. assuming that the wind and waves act simultaneously on the structure) dynamic analysis of wind and wave loadings was performed.

A number of 10 simulations were performed for each mean wind speed. Of course, the above number might be small for some of the more variable wind-wave states, but it was selected as a preliminary value due to the large computational effort that the process requires. At the end of each simulation, 10-minute time-series of reaction forces, moments, deflections and other values on the structure were obtained. Based on those time-series, the 10-minute stress history, by incorporating the reaction forces and moments were calculated for the cross-section of interest. As far as the geometry of the cross-section is concerned, the diameter was kept equal to 6 m (as in the standard model) and values from the range between 25 mm to 60 mm (with a step of 5 mm) were examined for the thickness. Rainflow counting and the Palmgren-Miner rule were used for the calculation of the 10-minute fatigue damage. Two different classes of detail, namely 40 MPa and 71 MPa, were assumed for the welded connection and the corresponding S-N curves of EC3 part 1.9 were employed. The Wöhler coefficients (which represent the slope of S-N curve) are equal to m=3 and m=5 as shown in Figure 3. According to EC3, a detail of 40 MPa corresponds to fillet welds, while a detail of 71 MPa corresponds to butt welds for connecting a circular hollow section to a ring-shaped flange plate.

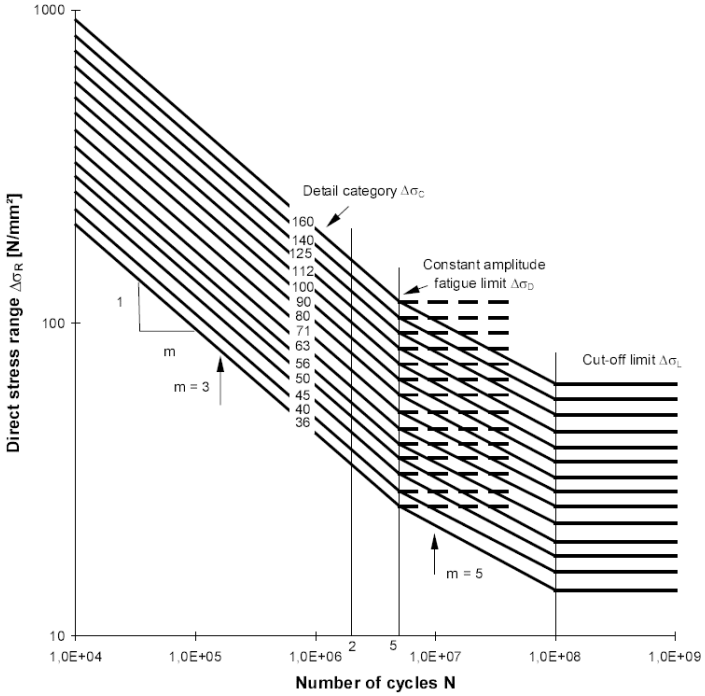

Figure 3: S-N curves for steel from EC3 Part 1.9.

From the above process, 10 potential values of 10-min fatigue damage were estimated for each of the selected wind speeds. Based on those 10 values the empirical cumulative density function of damage for each of the wind speeds was calculated and thus the empirical distribution of the damage was specified. For intermediate values of wind speed linear interpolation was used for determining the corresponding fatigue damage distribution.

The final step was to estimate the annual damage based on the 10-minute damage and the distribution of the annual wind speed data. Once the annual damage is calculated, the estimated fatigue life in years is equal to the reciprocal of that value. The process of calculating the annual damage (and the corresponding fatigue life) can be repeated numerous times since the distributions of the fatigue damage and the anemological data of the site are known. Thus, a Monte Carlo simulation for 100 years was performed in this study, in order to estimate the distribution of the fatigue life in the cross-section of interest. The results of this simulation for both sites and details of connection will be presented in the next section of the paper.

5 ANALYSIS RESULTS

5.1 Case 1: North Aegean Sea

The first site that was examined is in the north part of the Aegean Sea. The distribution of the 10 min mean wind speed at 10m (U_{10}) of the MSL in a typical year is shown in Figure 4. A statistical analysis also showed that the mean value of wind speed was 5.41 m/s and the standard deviation 2.92 m/s. Furthermore the distribution of the wind speed is best modeled by a lognormal distribution with parameters $\mu = 1.56$ and $\sigma = 0.51$. Regarding the wind direction, North-East (24.6%) and North (12.9%) constitute the preferred directions of winds in a typical year. Finally, as for the surrounding geometry, Table 1 shows the values of fetch for each of the eight main directions considered in this study.

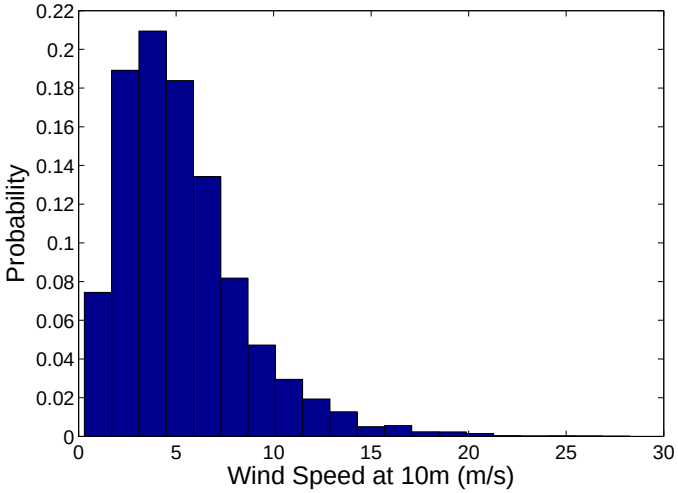

Figure 4: Distribution of non-zero 10 min mean wind speed at 10 m height (North site). There is also a ~30% probability of zero wind occurrence.

Direction	Fetch (Km)
N	5.8
NE	6.0
E	8.8
SE	34.4
S	73.1
SW	113.6
W	86.2
NW	18.9

Table 1: Fetch for each of the directions considered (North site).

The next step in the analysis was to estimate the joint PDF $f(H_s,U_{10})$ of wind speed and significant wave height. The joint PDF is calculated by the following formula:

$$f(H_s, U_{10}) = f_{H_s/U_{10}}(H_s/U_{10}) f_{U_{10}}(U_{10}) \tag{4}$$

where: $f_{U10}(U_{10})$ is the PDF of U_{10}, which is assumed to follow a lognormal distribution, as mentioned above and $f_{Hs/U10}(H_s/U_{10})$ is the conditional PDF of significant wave height H_s given the wind speed U_{10}. The distribution of the conditional PDF during a given storm is assumed to follow a Rayleigh distribution according to IEC 61400-3.

Using Eq. 4, the joint probability between wind speed and significant wave height can be estimated and the associated probability plots can be constructed. Since, the PDF takes into account two variables its plot is depicted as a surface in 3Dor in a 2D contour plot. Figure 5 shows a contour plot of the joint PDF for the North site studied. It is noteworthy that in Figure 5, the part of the contours associated with higher H_s corresponds to South directions, where the fetch is higher according to Table 1. This is because according to JONSWAP methodology the higher the fetch the larger is the H_s for a specific U_{10}.

From the specific PDF, one can determine the directions with the higher contribution for different wind speed values. The direction with the highest contribution for wind speed values up to 15 m/s at hub height (U_{90}) was the North-East (NE), and the North (N) direction for

speed values larger than 15 m/s. As shown in Table 1, the aforementioned directions are associated with fetch of 5.9 km and 5.8 km, respectively. Based on these values, the wave characteristics for each speed were calculated, and as expected they are practically negligible. The results are shown in Table 2.

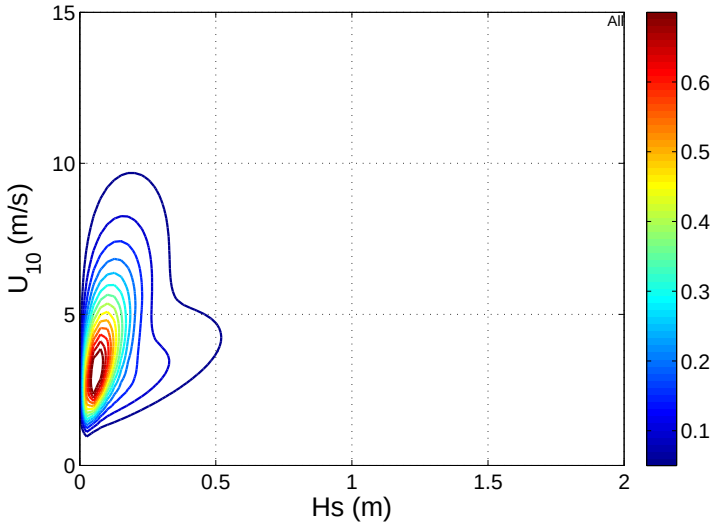

Figure 5: Contour plot of the joint PDF $f(H_s,U_{10})$ (North site).

A power-law wind profile (IEC 61400-3) was assumed for the distribution of the value of wind speed along the height z. According to this, if the wind speed is known at specific height z_0, the wind speed at height z is given by the formula:

$$U(z) = U(z_0)\left(\frac{z}{z_0}\right)^{\alpha} \tag{5}$$

where: α is the power-law exponent, taken to be equal to 0.14, as proposed by IEC 61400-3 for normal wind conditions. For the case at hand, z_0 = 10 m (reference value) and z = 90 m (hub height).

U_{90} (m/s)	U_{10} (m/s)	T_p (s)	H_s (m)	Dominant Direction	Fetch (km)
3	2.21	1.26	0.08	NE	6.0
5	3.68	1.50	0.12	NE	6.0
10	7.35	1.93	0.20	NE	6.0
15	11.03	2.24	0.30	NE	6.0
20	14.70	2.48	0.40	N	5.8
25	18.38	2.70	0.48	N	5.8
30	22.06	2.90	0.52	N	5.8

Table 2: Wind speed and wave characteristics at the North site.

The values of wind speed at hub height and the corresponding wave characteristics constitute the input to FAST, where the coupled dynamic analysis was performed. At the end of each simulation, time-series of stress history were obtained. A typical form of those time-series is shown in Figure 6. The stress time-histories are used in the estimation of fatigue damage and the corresponding fatigue life for the different wind speed values following the methodology of EC3 part 1.9 as mentioned in the theoretical background of this paper. Thus,

the annual fatigue damage and the corresponding fatigue life could be estimated. To this end, a simple Monte Carlo simulation was performed and 100 possible values of annual fatigue damage and corresponding fatigue life were calculated for each of the two details and for the different values of thickness for the cross-section of study.

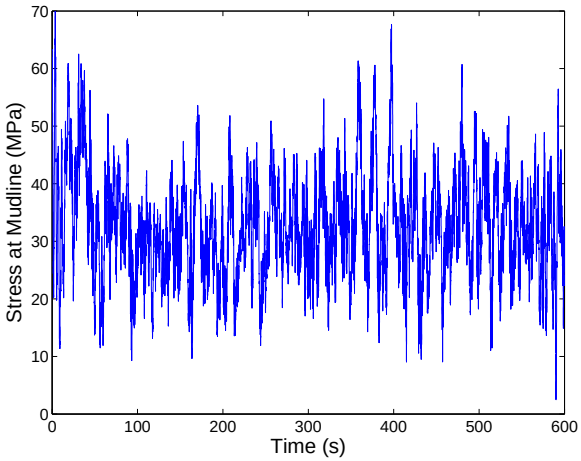

Figure 6: Typical form of stress time-series.

Table 3 shows the results of the analysis for the characteristics of the North Site. In specific, the average values of the annual damage and the corresponding estimated fatigue life for both types of detail, as resulted from the Monte Carlo simulations of 100 years are listed. An interesting finding is that the thickness of the cross-section has a significant effect on the annual damage for both details. In specific, as the thickness increases the annual damage decreases. This trend makes an intuitive sense, since a cross-section with larger thickness is expected to tolerate greater loads and be less vulnerable to fatigue. For instance, for a detail of 40 MPa, the annual damage of a cross-section with 25mm of thickness is around 40 times greater than a cross-section with 60 mm of thickness. The results are also plotted in Figure 7.

Thickness (mm)	DETAIL 40 MPa		DETAIL 71 MPa	
	Annual Damage	Fatigue Life (yrs)	Annual Damage	Fatigue Life (yrs)
25	0.1519	6.58	0.0159	63.06
30	0.0801	12.48	0.0064	156.76
35	0.0449	22.26	0.0026	382.21
40	0.0262	38.16	0.0011	936.09
45	0.0156	64.29	4.043E-04	2473.80
50	0.0094	106.24	1.562E-04	6403.04
55	0.0057	174.55	4.839E-05	20671.37
60	0.0035	285.91	1.337E-05	74830.91

Table 3: Results of Analysis for the North site

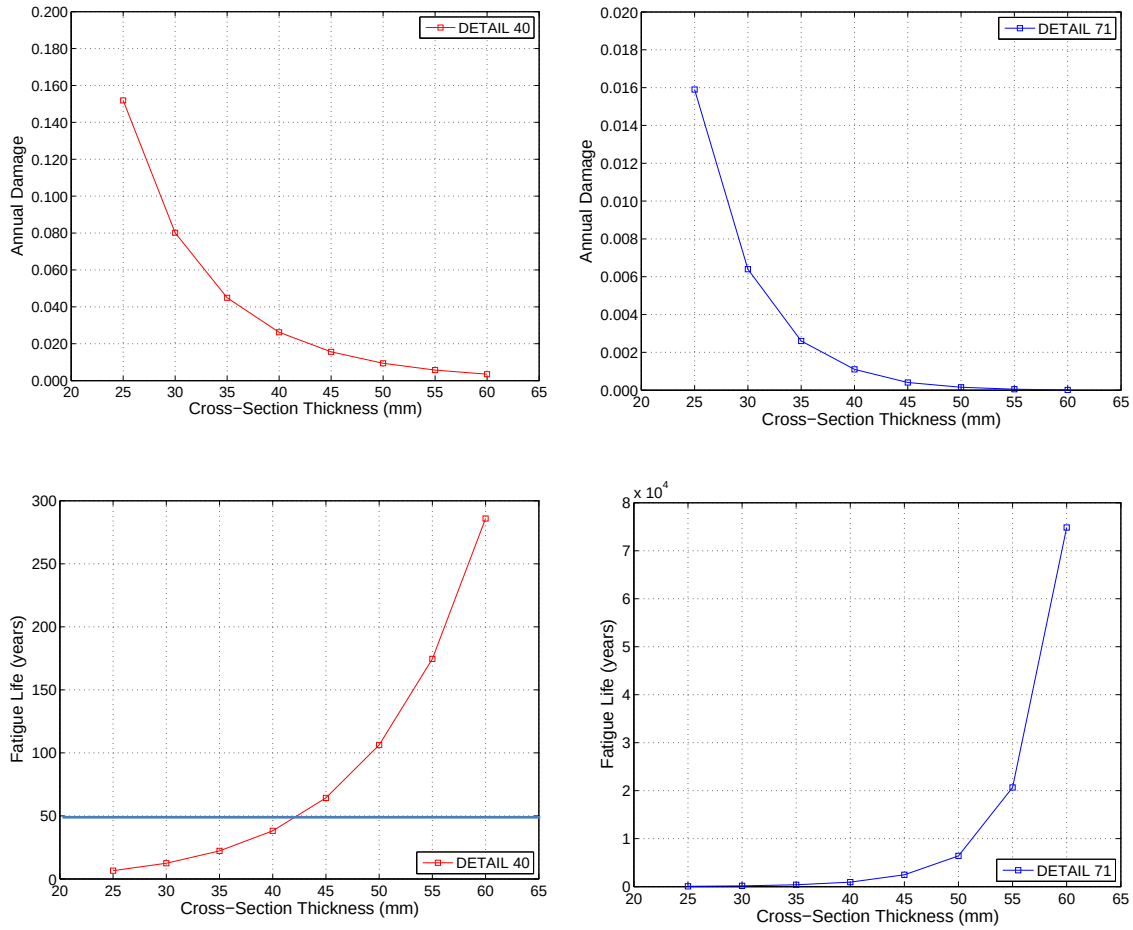

Figure 7: Annual damage and thickness of cross-section (top graphs) and fatigue life and thickness of cross-section (bottom graphs) for North site

The annual damage is directly associated with the fatigue life. As mentioned in a previous subsection, the fatigue life is approximately equal to the reciprocal of the annual damage. From the results listed in Table 3, an inference is that the fatigue life (which is a more tangible magnitude in common sense than damage, since it is measured in years) depends highly on the thickness of the cross-section. In specific, regardless of the detail, as thickness increases the expected fatigue life increases as well. Of course, this finding is intuitively expected, since a long fatigue life is associated with low annual damage.

It is noteworthy that the estimation of the fatigue life may be of special interest during the design phase of an offshore wind turbine. In other words, based on the expected fatigue life the designer is able to select an appropriate thickness for the pile's cross-section. This is because, it could be estimated whether a specific selection of thickness and detail of connection will make the specific cross-section to last during the whole design life of the structure. For example, in the case of an offshore wind turbine the structure's life-time is usually considered to be equal to 50 years. Based on the values of Table 3, one could conclude that if a detail of 40 MPa is selected, the minimum thickness that is expected to last longer than the design life (with respect to fatigue) is 45 mm. If a thickness less than 45 mm is used, then a fatigue failure is expected sooner than the end of the design life, i.e. during the service life of the wind turbine. For this reason a horizontal line is plotted in the bottom left graph of Figure 7 at the level of 50 years. The role of this line is to graphically show the above inference.

On the other hand, if a detail of 71 MPa for the welded connection is used, then no fatigue failure is expected during the life of the wind turbine, even if a thickness of 25 mm is used. This is because a thickness of 25 mm is associated with a fatigue life of around 63 years that is greater than 50 years. It is also noteworthy that if a thickness of more than 40 mm is used, then the fatigue life is estimated to be thousands of years. The latter means that no fatigue failure is expected in those cases. However, the benefit of the absence of fatigue may be associated with a high price such as higher construction costs (larger cross-section, advanced welded connection).

5.2 Case 2: South Aegean Sea

The second site of this study was selected to be in the South Aegean. It was also assumed that this site is far enough from shore in order to use the same fetch (equal to 120 km) regardless of direction. This assumption is of course oversimplified but it has the advantage that it does not require the consideration of wind direction in the analysis. At this point, the authors would like to mention a legal limitation that may arise. As of today, Greece has not declared an Exclusive Economic Zone and its territorial waters are extended up to 6 nautical miles from the shore. Thus, any planned offshore wind farm would have to be placed inside the above 6-mile zone. For this reason, a site with such a large omnidirectional fetch may not yet be available for exploitation in the Aegean Sea. However, the authors performed an analysis in order to evaluate the effect of a duration-limited (rather than fetch-limited) sea state. When the regional politics will allow it, such a case can become more of a practical, rather than a theoretical possibility.

Figure 8 shows the distribution of the wind speed at 10 m at the South site. A statistical analysis showed that the mean value of the wind speed is equal to 7.74 m/s and the standard deviation is equal to 5.10 m/s. Thus, a first inference is that South site is characterized by higher wind speeds than the North site. Finally, it was found that a Weibull (and not a lognormal) distribution with parameters $\lambda = 8.65$ and $k = 1.58$ provides the best fit.

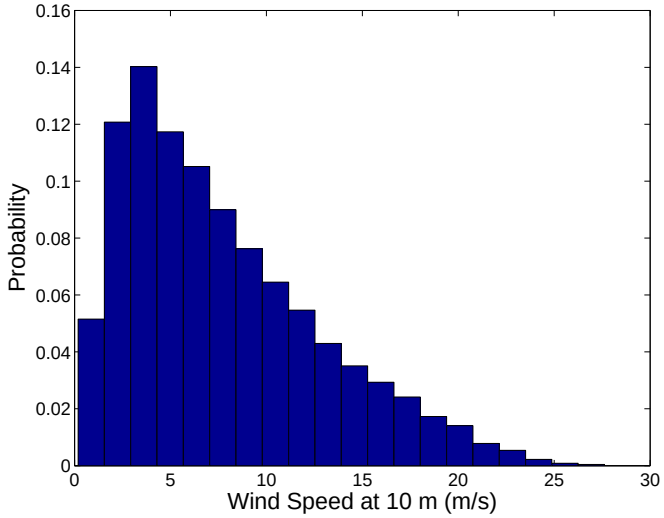

Figure 8: Distribution of Wind Speed at 10 m height (South site).
The zero-wind probability is practically zero.

The same assumptions and analysis process as in the case of the North site were undertaken for the estimation of the fatigue damage. Table 4 shows the wind speed and wave characteristics that were used for the dynamic analysis. From Table 4 it becomes obvious that, as expected, the wave intensity characteristics are quite more significant compared to those of

the North site. Of course this can be attributed to the longer fetch distances that were employed. Fig. 10 shows the contour plot of the joint PDF $f(H_s,U_{10})$ for the South site. Now, all contours have an "oval" shape since the same fetch is assumed for all directions. In the North site, only South and South-East winds are practically fetch-unlimited, but generally less frequent, this leading to the lower-right lobe appearing in Figure 5 that is absent from Figure 9.

U_{90} (m/s)	U_{10} (m/s)	T_p (s)	H_s (m)	Fetch (km)
3	2.21	3.42	0.36	120
5	3.68	4.08	0.59	120
10	7.35	5.23	1.24	120
15	11.03	6.08	1.94	120
20	14.70	6.78	2.70	120
25	18.38	7.40	3.50	120
30	22.06	7.96	4.36	120

Table 4: Wind speed and wave characteristics at the South site

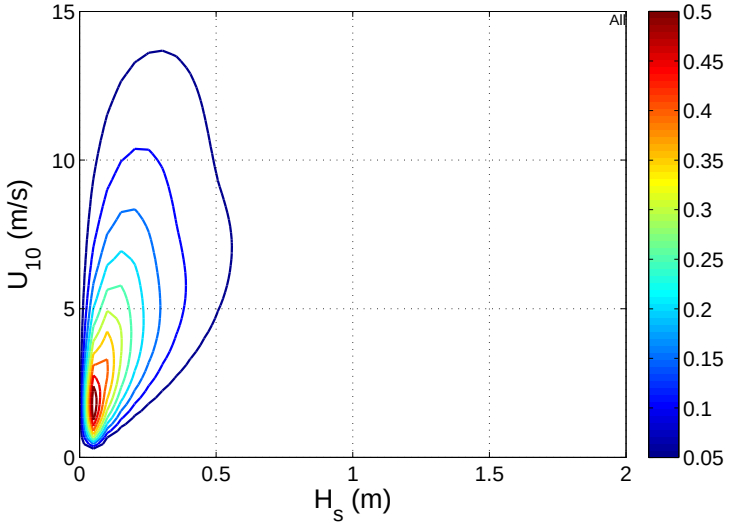

Figure 9: Contour plot of the joint PDF $f(H_s,U_{10})$ at the South site.

The Monte Carlo analysis gave the results shown in Table 5. The results, as expected, follow the same trends as in the case of the North site. However, due to the higher wind and wave conditions of the site, very large values of annual damage and low values of fatigue life were calculated. It is noteworthy that for a detail of 40 MPa, only if a thickness of 60 mm is used, the fatigue life will be slightly greater (only about 6 years) than the design life. For this reason only the combination associated with 60 mm of thickness is above the reference line of 50 years in the bottom left graph of Figure 10. For lower values of thickness a detail of 40 MPa will give fatigue lives lower than 50 years. Moreover, for very low values (lower than 40 mm) the estimated fatigue life is lower than 10 years.

If a detail of 71 MPa is selected, then longer values of fatigue life are expected. However, it should be mentioned that even with the better detail, only if the thickness of the cross-section is larger than 30 mm, the estimated fatigue life is greater than the design life of the wind turbine. Finally, if a value of thickness larger than 50 mm is used then the estimated fatigue is greater than 500 yrs (10 times the design life) and no fatigue failure is expected in practice.

Thickness (mm)	DETAIL 40		DETAIL 71	
	Annual Damage	Fatigue Life (yrs)	Annual Damage	Fatigue Life (yrs)
25	0.5791	1.73	0.0687	14.55
30	0.3130	3.20	0.0304	32.91
35	0.1812	5.52	0.0139	72.02
40	0.1087	9.20	0.0064	157.20
45	0.0676	14.80	0.0031	326.10
50	0.0429	23.29	0.0015	674.38
55	0.0276	36.20	0.0007	1394.30
60	0.0179	55.77	0.0003	3048.30

Table 5: Results of Analysis for the South site.

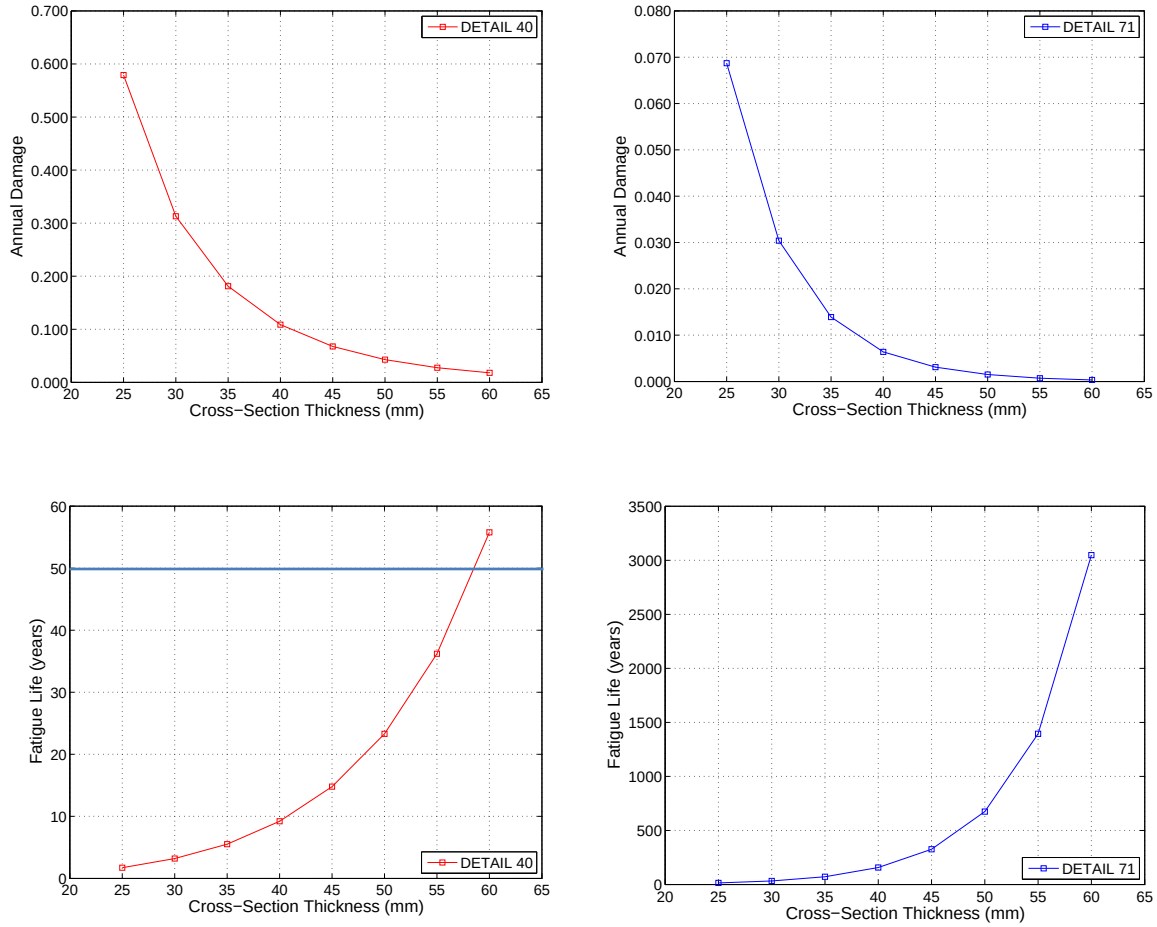

Figure 10: Annual damage and thickness of cross-section (top graphs) and fatigue life and thickness of cross-section (bottom graphs) for South site

5.3 Discussion of findings

Based on the results of both sites, it is inferred that for the site with higher wind and waves (South site) larger fatigue damage is expected for all the values of thickness examined in this study. This finding is associated with shorter fatigue life for the cross-section of interest. This certainly makes sense since larger wind and wave loads are expected to act on the construc-

tion. Finally, as expected, the lower-quality fillet welds (detail 40 MPa) are more vulnerable to fatigue than butt welds. Figure 11 shows that for the case of the South site a fillet weld might not be appropriate since it will result to a fatigue failure before the end of the design life of the wind turbine (with only exception the case of 60 mm thickness). Furthermore, even in the case of North site, where the wind and waves are milder, the use of a fillet weld requires at least 45 mm of thickness in order to last during the whole design life.

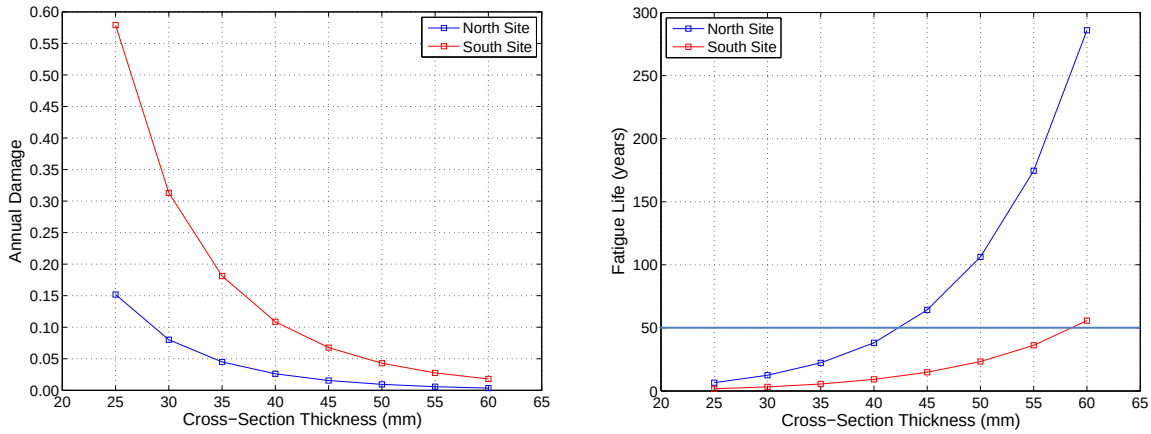

Figure 11: Comparison of annual damage (left graph) and fatigue life versus thickness of cross-section (right graph) for fillet welds (detail 40MPa) for the examined sites

On the other hand, the use of butt welds is found to be a safe (albeit expensive) solution regardless of thickness for the North site, since the expected fatigue life is longer than the design life, even when the smallest thickness is used. For the South site though, the use of butt weld requires a minimum with of 35 mm (see Table 5) in order the fatigue life to be longer than the design life.

The inferences from the above discussion may be useful, especially during the design of the foundation pile. Fillet welds might not be appropriate in a construction site characterized by windy conditions, however they might be a potential cost-reduction technique for sites with less intensive wind loads, since they are much cheaper to execute than butt welds and with an appropriate thickness may last more than the design life.

6 CONCLUSIONS

In this paper, a probabilistic fatigue life assessment for a standard offshore wind turbine with a monopile design was presented. Two potential sites of construction in the Aegean Sea of Greece with different wind and wave characteristics were examined. A fully coupled dynamic analysis for the calculation of loadings due to wind and wave was performed using the freely available FAST software. The assessment of fatigue damage (and corresponding fatigue life) was made considering two different details of welded connections according to EC3 for the cross-section at mudline of the structure.

The results follow the obvious trends: Turbines at windier sites with longer fetch distances are obviously more vulnerable to fatigue. Lower quality fillet welds similarly attract higher fatigue damage compared to more expensive butt welds. The thickness of the cross-section is a crucial parameter for the design, since a small thickness may result in a very quick fatigue failure, especially in the case of fillet welds.

Finally, as an overall conclusion of this work is that the accuracy offered by a detailed probabilistic approach can help in properly quantifying the actual performance of the structur-

al components and thus result to a better compromise between safety and economy. Incorporating further sources of uncertainty and operational states of the wind turbine (e.g., starting and stopping) will only improve the accuracy in such predictions and help offer a cost-effective custom-made solution for a site of interest.

ACKNOWLEDGEMENTS

This research has been co-financed by the European Union (European Social Fund - ESF) and Hellenic national funds through the Operational Program "Competitiveness and Entrepreneurship" of the National Strategic Reference Framework (NSRF 2007-2013) - Research Funding Program: Bilateral R&D Cooperation between Greece and China 2012-2014.

REFERENCES

[1] J.D. Sorensen, Reliability Analysis of Wind Turbines Exposed to Dynamic Loads. A. Cunha, E. Caetano, P. Ribeiro, G. Muller eds. *9th International Conference on Structural Dynamics*, EURODYN 2014, Porto, Portugal, 2014.

[2] J.M. Jonkman, Dynamics of Offshore Floating Wind Turbines-Model Development and Verification. *Wind Energ.* **12**, pp.459-492, 2009

[3] T. Moan, Stochastic Dynamic Response Analysis of Offshore Wind Turbines in a Reliability Perspective. A. Cunha, E. Caetano, P. Ribeiro, G. Muller eds. *9th International Conference on Structural Dynamics*, EURODYN 2014, Porto, Portugal, 2014.

[4] P. Passon, K. Branner, Condensation of Long-Term wave Climates for the Fatigue Design of Hydrodynamically Sensitive Offshore Wind Turbine Support Structures. *Ships and Offshore Structures*, Taylor & Francis, 1-25, 2014.

[5] S.R. Arwade, M.A. Lackner, M.D. Grigoriu, Probabilistic Models for Wind Turbine and Wind Farm Performance. *ASME Journal of Solar Energy Engineering*, **133**, No. 4: 041006, 2011.

[6] J. Jonkman, S. Butterfiled, W. Musial, G. Scott, Definition of a 5-MW Reference Wind Turbine for Offshore System Development. *Technical Report NREL/TP-500-38060. NREL Technical Report*, National Renewable Energy Laboratory, Golden, Colorado, 2009.

[7] H.J.T. Kooijman, C. Lindenburg, D. Winkelaar, E.L. van der Hooft, DOWEC 6 MW Pre-Design. *Tech Report DOWEC-F1W2-HJK-01-046/9 (Public Version)*, Petten, Holland, 2003.

[8] IEC 61400-3, Wind Turbines-Part 3: Design Requirements for Offshore Wind Turbines. *European Committee for Electrotechinal Standardization*, Brussels, Belgium, 2009.

[9] DNV-RP-C205, Environmental Conditions and Environmental Loads. *Det Norske Veritas*, Bærum, Norway, 2010.

[10] B.J. Jonkman, L. Kilcher, TurbSim User's Guide: Version 1.06.00. *Tech Report NREL/EL-xxx-xxx (Draft Version)*, National Renewable Energy Laboratory, Golden, Colorado, 2012.

[11] J.D. Jonkman, M.L. Kilcher Jr, TurbSim User's Guide: Version 1.06.00. *Tech Report NREL/EL-xxx-xxx (Draft Version)*, National Renewable Energy Laboratory, Golden, Colorado, 2005.

[12] J. Morison, M.P. O'Brien, J.W. Johnson, S.A. Schaaf, The Force Exerted by Surface Waves on Piles. *Petroleum Transactions*, **189**, 149-154, 1950.

[13] Eurocode 3: Design of Steel Structures, Part 1.9: Fatigue Strength of Steel Strutcures.

CEN Central Secretariat, Brussels, Belgium, 2002.

[14] ASTM E1049-85, Standard Practices for Cycle Counting in Fatigue Analysis. *Annual Book of ASTM Standards*, 03.01, 710-718, 1997

[15] A. Nielsony, Determination of Fragments of Multiaxial Service Loading Strongly Influencing the Fatigue of Machine Components. *Mechanical Systems and Signal Processing*, **23**, 2712-27121, 2009

[16] MedPAN, Overview of Planned OWF Projects in the Mediterranean. *Network of Marine Protected Area Managers in the Mediterranean*, Marseille, France, 2013.